Scale Invariance, Symmetries, Fractals, and Stochastic Simulations of Atmospheric Phenomena

S. Lovejoy[1] and D. Schertzer[2]

Abstract

Advances in remote sensing and in situ measurement techniques have revealed the full continuum of atmospheric motions and have underlined the importance of mesoscale processes. This paper examines the implications of three observed characteristics of mesoscale circulations: 1) the energy spectrum of the horizontal wind in the horizontal is of the form $k^{-\beta_h}$ with $\beta_h \sim 5/3$, (k is a wavenumber); 2) the corresponding spectrum in the vertical direction is of the same scaling form, but with a very different slope ($\beta_v \sim 11/5$); and 3) the variability is extreme.

Some recent work in turbulence, physics, and meteorology, that is relevant to systems with extreme variability over a wide range of scales is reviewed. The concepts of scaling, intermittency, and fractals, are briefly introduced to show how they can be used to understand the physics of both homogeneous and intermittent energy cascades in isotropic atmospheres. These concepts may be generalizable (with a formalism called generalized scale invariance), to account for atmospheric intermittency and especially for anisotropy.

Finally, it is shown how to construct fractal models.

These models are useful because they produce realizations of random fields that are broadly of the same sort as those that may be allowed by the equations, while at the same time depending on empirically determined parameters. This enables them to retain close links with both the data and the physics. Finally, possible applications in mesoscale modeling, sampling problems, remote sensing, nowcasting, hydrology, and numerical weather prediction (NWP) systems are briefly discussed.

1. Introduction

Interest in atmospheric dynamics has traditionally been concentrated at two poles: the immediately perceived small turbulent scale and the large synoptic scale accessible via conventional observing networks. It wasn't until the fifties and sixties, when radar and then satellites opened up the new realm of the "mesoscale," that meteorologists were directly confronted with the full continuum of atmospheric phenomena.

Remotely sensed and modern in situ data have now revealed that far from being a dull energy sink (associated with a hypothetical "gap" in the spectrum—e.g. Van der Hoven, 1957), the mesoscale is both active and interesting. There is now general agreement about the following basic aspects of the mesoscale (see Schertzer and Lovejoy [1983, 1985a] and especially the valuable review by Lilly [1983]):

1) *Scaling.*[3] Fluctuations occur over a wide range of time and space scales: in particular, the energy spectrum of the wind in the horizontal is of the scaling (power-law) form $k^{-\beta_h}$ where k is a wavenumber and β_h is a (horizontal) exponent of value ~5/3.
2) *Anisotropy.* For heights up to at least 5 km, the corresponding (horizontal) wind spectrum is also scaling but is quite different from the horizontal ($\beta_v \sim 11/5$).[4] Over this range, the anisotropy introduced by gravity is therefore independent of scale.
3) *Extreme variability.* This is mostly due to sparsely distributed active regions that account for most of the energy and moisture flux (see e.g. Wyngaard, 1983).

In the following, work on scale invariance and intermittency in isotropic systems is first reviewed, and a brief outline of a symmetry principle called generalized scale invariance (GSI), which constitutes a systematic extension of these concepts to anisotropic situations, is given.

Most of the results presented have been published elsewhere, hence, this article's organization is primarily directed to simply and clearly explaining the main ideas, many of which are more familiar to physicists than to meteorologists. The exposition therefore follows a somewhat indirect path, relying on the extensive use of elementary stochastic models of cascade processes. While the first few examples are clearly only for pedagogical purposes, the later ones are already sufficiently realistic so as to deserve study in their own right. These models are useful because they produce realizations of random fields that are broadly of the same sort as those that may be allowed by the equations, while at the same time depending on empirically determined parameters. This enables them to retain a close link with both the data and the basic physical principles. We briefly discuss how they can be ap-

[1] Physics Department, McGill University, 3600 University St., Montreal, Quebec H3A2T8, Canada.

[2] EERM/CRMD, Meteorologie Nationale, 2 avenue Rapp, 75007 Paris, France. Current address: Physics Department, McGill University, 3600 University St., Montreal, Que. H3A2T8, Canada.

[3] A specific type of scaling may be defined for the one-dimensional function $X(t)$ as follows: $\Delta X(\lambda \Delta t) \stackrel{d}{=} \lambda^H \Delta X(\Delta t)$, where $\Delta X(\Delta t) = X(t_0 + \Delta t) - X(t_0)$, $X(\lambda \Delta t) = X(t_0 + \lambda \Delta t) - X(t_0)$, is a scale ratio and the equality is understood in the sense of probability distributions (i.e., $X \stackrel{d}{=} Y$ if $Pr(X > q) = Pr(Y < q)$ for all q; Pr means probability). This equation states that fluctuations at large scale ($\lambda \Delta t$, $\lambda > 1$) are related to those at small scale (Δt) by the constant factor λ^H. Note that for finite variance, $\beta = 2H + 1$. Most experimental tests of scaling have involved statistical averages over large ensembles. However, if the probability distribution is "fat-tailed" (intermittent, see Section 2c), then in specific situations (such as storms) large deviations from the mean (e.g. random spectral peaks) will occur.

[4] 11/5 is the value obtained from dimensional arguments as well as from a number of empirical studies (see the discussion in Schertzer and Lovejoy, 1985a). Although the exact value may be debated, there is general agreement that $\beta_v > \beta_h$, which is all that we require here.

plied in mesoscale modeling, sampling problems, remote sensing, nowcasting, hydrology, climatology, and numerical weather prediction (NWP) systems. Finally, it is suggested how these simple models can be improved so as to represent meteorological phenomena more accurately.

2. The physics of atmospheric cascades

a. *Atmospheric symmetry principles*

Modern physics has developed largely through the systematic use of symmetry principles. A system is *symmetric* when it is invariant under a certain group of transformations that may be much more abstract than simple mirror or rotational symmetries. The familiar meteorological symmetry principles are the invariance (or conservation) of energy, momentum, and matter. What is missing, and what an explicit set of equations such as the Navier-Stokes equations ought to provide, is an additional symmetry that determines the aspects of atmospheric structures that are invariant with respect to changes in scale. Symmetries of this sort are called scale invariance (abbreviated to scaling). It is a telling commentary on the difficulty of the subject that more than 40 years after the prediction that the Navier-Stokes equations should lead to scaling spectra, there is still no solid proof. However, very few doubt that the connection is real and many nonrigorous arguments exist. For some recent numerical results, see Chorin (1981) and Brachet *et al.* (1983).

There are now a large number of measurements (mainly of spectra) which support the idea that over a large fraction of meteorologically significant scales, the atmosphere is scaling (see the references in Lilly [1983] and Schertzer and Lovejoy [1985a]). Over their range of validity, power-law spectra are scaling because they do not involve characteristic lengths. Strong evidence (complementary to that obtained from spectra) for the existence of scaling is Lovejoy's 1982 study of the "complexity" of cloud and rain areas (A) and perimeters (P). From at least 1 to 1000 km, the scaling relation $P/P_s = (A/A_s)^{D_P}$, where P_s is the linear and A_s the areal resolution of the sensor, was found to hold with $D_P \sim 1.35$. D_P is the fractal (see below) dimension of the perimeter (=1 for smooth lines, and =2 for maximally complicated curves that literally fill the plane). The lower limit has been extended with *Landsat* imagery by Cahalan *et al.* (1984) to 0.16 km.

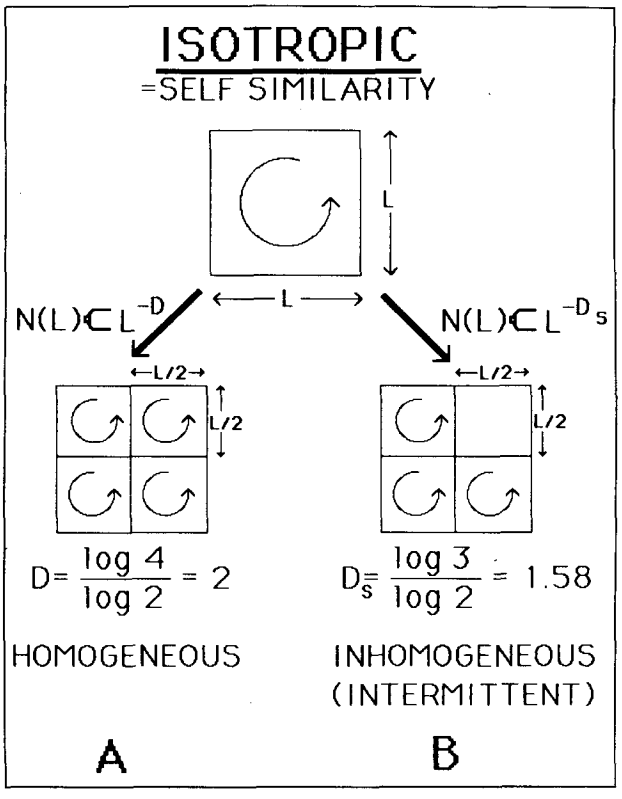

FIG. 1. Schematic representation of how various isotropic-turbulence models treat the breakup of an eddy (represented by the square) via nonlinear interactions during a single step in the cascade process. The various schemes are divided into homogeneous and inhomogeneous (intermittent). The formula giving the number of active eddies at size (L) [$=N(L)$] is shown. D_s is the dimension characterizing the "sparseness" of the support.

b. *Turbulence in isotropic atmospheres*

In the simplest scale invariance of interest, "self-similarity," the statistical properties of the large scale are simply magnified carbon copies of those at small scales. Although at first sight trivial, self-similarity is in fact compatible with a bewildering variety of shapes, as graphically illustrated by the beautiful illustrations of self-similar fractals in Mandelbrot (1982).[5] He has also convincingly shown that many physical systems such as the earth's topography, coastlines, and rivers are fractals. It is worth noting that the scale invariance of these atmospheric boundary conditions—as well as that of others such as the solar forcing—(insolation; Gauthier, private communication, 1983) are important in accounting for the observed power-law wind spectra.

It is therefore perhaps not very surprising that the earliest turbulent scheme of atmospheric motions (Richardson, 1922, 1926) was generated by a self-similar series of steps in which eddies of a given size are broken up by the nonlinear interactions into smaller sizes. The smaller (sub) eddies are in turn broken up and the process is repeated until scales small enough for viscosity to be important are reached. At each step in this isotropic, homogeneous cascade,[6] the energy is transferred (without dissipation) from the larger to the smaller eddies: it is thus an invariant of the cascade. This process is shown schematically in Fig. 1. The initial eddy, represented for convenience by a square, is transformed by a single cascade step. Each of the subeddies are copies of the original reduced by the linear ratio λ (here taken =2) and each containing a fraction λ^{-2} of the original energy. If this process is continued indefinitely, it is clear that the energy distribution is statistically homogeneous and isotropic. This

[5] The expression *fractal* was originally coined to denote shapes having the property that a fragment is similar to the whole. We continue to use this term in the context of anisotropic phenomena (GSI—see section 3), although it is clear that here the part may require a deformation and/or rotation in order to resemble the whole (see the discussion in Schertzer and Lovejoy, 1984b).

[6] The terms *homogeneous* and *isotropic* refer respectively to translational and rotational invariance.

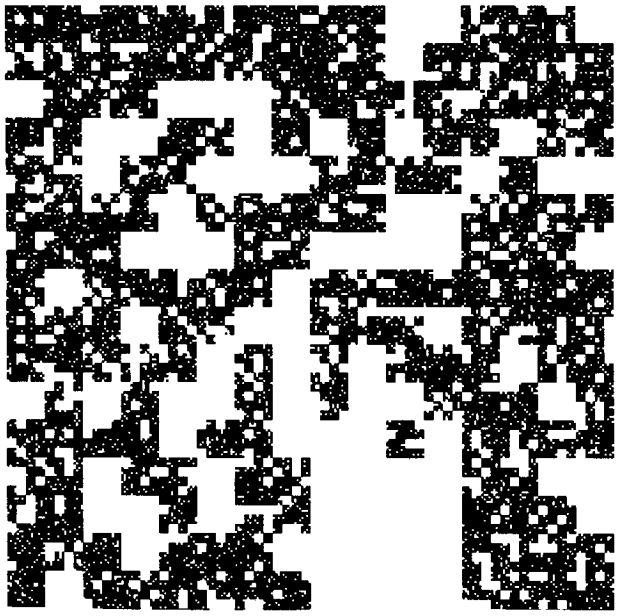

FIG. 2. The simple cascade scheme on a square grid corresponding to Fig. 1B (but with $\lambda = 4$). For each "subeddy" thus generated, choose a random number uniformly distributed over the interval (0, 1). If it exceeds some pre-assigned value ($p = 0.70$ in this case), the eddy is considered "dead" (shown as white); otherwise it survives (black), there being N survivors per generation. The average number of survivors $\langle N \rangle$ is $\lambda^2 p = 16 \times 0.7 = 11.2$. When the cascade process is iterated an infinite number of times (here it is followed for only four generations on a 256×256 point grid). The set of surviving "active" regions has dimension $D_s = \log \langle N \rangle / \log \lambda = \log 11.2 / \log 4 = 1.73$.

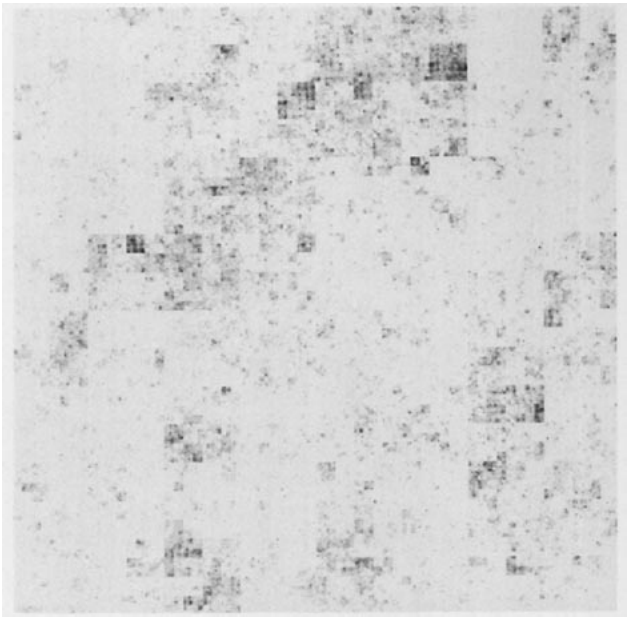

FIG. 3. The α-model with $\lambda = 2$ and nine cascade steps on a 512×512 grid with $D_s = 1.98$ and $D_\infty = 1.5$. The logarithm of the energy flux ϵ is indicated by the grey shading—weak regions white (however there are no completely "dead" regions) and intense regions black. If a threshold is fixed, the set of points exceeding it will look something like that shown in Fig. 2 (i.e. $D_s < 2$) with the difference that the actual value of D_s is now a function of the threshold. The model is therefore "multidimensional." It is also hyperbolically intermittent since spatial averages of the invariant measure ϵ have hyperbolic distributions.

simple scheme of homogeneous isotropic turbulence leads directly (via dimensional arguments) to Kolmogorov's (1941) $k^{-5/3}$ energy spectrum. Isotropic-cascade ideas have been so successful that the idea of self-similarity is now central to virtually all theories of turbulence.

c. The problem of intermittency

Kolmogorov assumed that all regions occupied by the fluid were equally active. However, it soon became clear that this was far from true: turbulence was recognized to be "spotty" or "intermittent" (Batchelor and Townsend, 1949), with active regions occupying only a small fraction of the space available. Attempts to account for this intermittency, via the work of Novikov and Stewart (1964) and Yaglom (1966), lead to a more general cascade scheme (Mandelbrot, 1974). The simplest case, (known as the β-model; Frisch *et al.*, 1978) is illustrated in Fig. 1b. As before, the large eddy is broken up isotropically. Now however, the subeddies are randomly chosen to be either "dead" or "alive" (active), with the energy at each step being divided equally only between the N active subeddies, with $\langle N \rangle < \lambda^2$ (in Fig. 1b, $N = 3$).[7] When the process of division into subeddies and redistribution of energy is iterated indefinitely, the energy is eventually distributed over a set of points such as that shown in Fig. 2 (called the "support" of the turbulence) which is a crude representation of the active regions of a two-dimensional section of an isotropic three-dimensional atmosphere. These regions are so "sparse" that the area occupied by them is zero. In fact the best way to characterize this "sparseness" is not by the area covered, but by the mathematical (Hausdorff, fractal) dimension[8] of the support $D_S = \log \langle N \rangle / \log \lambda$. In Fig. 2, $D_S = 1.73$; the set is therefore more than linelike ($D_S > 1$, so that its "length" is infinite) but less than arealike ($D_s < 2$, therefore, the area $= 0$).[9] If we were to determine the number of points within a radius L of a randomly chosen point on this figure, it would vary as L^{D_s}.[10] Note that by changing $\langle N \rangle$ we can obtain a set with any dimension between zero and the dimension of the underlying space (here =2). In fully developed three-dimensional isotropic turbulence, there is general agreement among experimentalists that $2.3 < D_s < 2.8$ (e.g. Antonia *et al.*, 1982). Turbulence is therefore difficult to apprehend because the (active) regions of greatest interest occupy a volume that, strictly speaking, is zero! Note that the

[7] Hereafter, angle brackets denote statistical averages, and overbars denote spatial averages.

[8] See Kahane (1976, 1985) for a mathematical introduction and discussion.

[9] The use of fractional dimensions is not as strange as it may seem. Everyone is familiar with the fact that the area of a line is zero and that a plane is infinitely "long." To obtain a positive but finite measure of a set, the correct dimension—in this case D_s—must be used.

[10] Note that D_s is not necessarily equal to D_p since D_s refers to a set that includes interior points, while D_p does not.

volume's being zero doesn't mean that the phenomenon in question is "small" (e.g. a plane is infinitely large, but of zero volume): the size must be determined using the correct (Hausdorff) dimension.

Having mastered this archetypal fractal construction, we are now prepared to consider an almost as simple, but much more instructive, example. Rather than dividing eddies into categories of dead or alive according to a certain probability, we characterize them as being either weak or very active. The energy in each subeddy is determined by multiplying that of the parent eddy by one of two fixed factors, the first of which is less than unity, the second greater than unity, the choice being made according to a predetermined probability level. The factors are constrained so that on average, the energy in the subeddies is equal to that in the parent eddies. This insures that the energy remains an invariant of the process. The result of this process, called the α-model in Schertzer and Lovejoy (1983, 1984a), is shown in Fig. 3.[11] In fact, in all cases except the β-model, the process has the following main properties:

1) No regions are completely "dead."
2) If a set of points exceeds a particular threshold, the dimension of this set gradually decreases as the threshold is increased. Eventually we obtain a very sparse set with dimension D_∞. The model is thus "multidimensional" (see Hentschel and Procaccia, 1983; Grassberger, 1983; Schertzer and Lovejoy, 1983; Mandelbrot, 1984a; Parisi and Frisch, 1984).
3) The probability distribution function, Pr, for intense regions is asymptotically hyperbolic:

$$\Pr(\bar{\epsilon}' > \bar{\epsilon}) \propto \bar{\epsilon}^{-\alpha_\epsilon} \text{ (for large } \bar{\epsilon}),$$

for the probability that a random (spatially averaged) energy flux $\bar{\epsilon}'$ exceeds a fixed threshold $\bar{\epsilon}$; α_ϵ is an exponent depending on the details of the construction and on the dimension of the region over which ϵ is averaged. The smaller the value of α_ϵ, the more intermittent the resulting field is, and the more extreme the fluctuations. In particular, the moments $\langle \bar{\epsilon}^h \rangle \to \infty$ if h is greater than or equal to α_ϵ (see discussion in Section 3b).

d. The problem of anisotropy

If self-similarity is assumed, and one extrapolates from a small roundish cloud, the absurd conclusion that clouds thousands of kilometers long may also be thousands of kilometers thick is quickly reached. Clearly, the vertical stratification of the atmosphere precludes the possibility that it is self-similar throughout. The classical scheme of atmospheric motions (e.g. Monin, 1972) attempts to avoid this difficulty

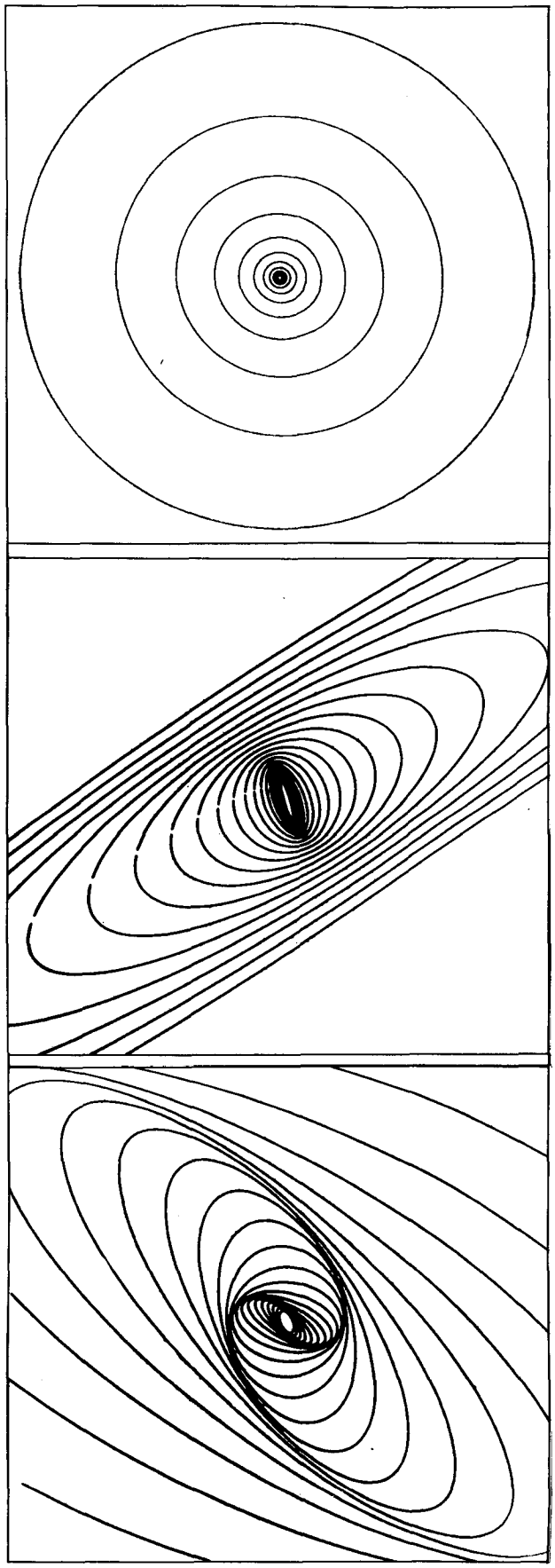

FIG. 4. (right) The shapes of the average eddies at different scales for (top) isotropic (self-similar) turbulence, (middle) anisotropic, horizontally stratified turbulence (a vertical cross section obtained after averaging over the different horizontal directions is shown). As scale size is increased, the horizontal axis of the ellipses (L) increases as L while the vertical axis increases as $L^{H_z} = L^{1+H_z} = L^{1.555}$, hence the dimension ($D_{el}$) is 1.555 rather than 2. (bottom) An example of both differential stratification and rotation (modeling the effect of the Coriolis force). Here, $D_{el} = 2$ in accord with observations in the horizontal.

[11] So called because of the exponent α that it introduces.

by postulating a three-dimensional self-similar regime at small scales and a two-dimensional self-similar regime at large scales. If they exist, these regimes would be totally different, because of the conservation of vorticity in two but not three dimensions. Furthermore, the boundary separating the two regimes would be marked by a sharp "dimensional transition" (Schertzer and Lovejoy, 1985a).

Following Schertzer and Lovejoy (1983, 1985a,b,c), it is clearly more natural to directly study anisotropic cascades. Such a study led to the surprising conclusion that the effective dimension of the atmosphere is neither two nor three, but rather the intermediate value $D_{el} = 23/9 = 2.555\ldots$. At larger and larger scales, the atmosphere becomes progressively "flatter" but is never two-dimensional. Figures 4a, b, c compare the shapes of the average eddies in the isotropic (self-similar) and some simple anisotropic cases (see the discussion in the next section). The dimension 2.555 is called an elliptical dimension because of the ellipsoids it introduces.

A schematic illustration of simple anisotropic cascades is shown in Fig. 5. Rather than producing subeddies by dividing both axes of the parent eddy by the same factor, we divide one by λ and the other by λ^{H_z}. Figure 5 shows this with $\lambda = 4$, $H_z = 1/2$. The resulting elliptical dimension is $1 + H_z = 1.5$; in the isotropic case it is 2. At each step in the process, the initial rectangular eddy is reduced in size and elongated. The transformation from one scale to another now involves a compression as well as a reduction (this process can obviously reverse itself and go from a small to a large scale, in which case the eddies "stretch" more and more and become more and more flat). Note that as in the atmosphere, the structures at the largest scales are the most horizontally stratified. In the atmosphere, theoretical and experimental results show $H_z = 5/9$, hence $D_{el} = 2 + H_z = 23/9$ (Schertzer and Lovejoy, 1983, 1985a).

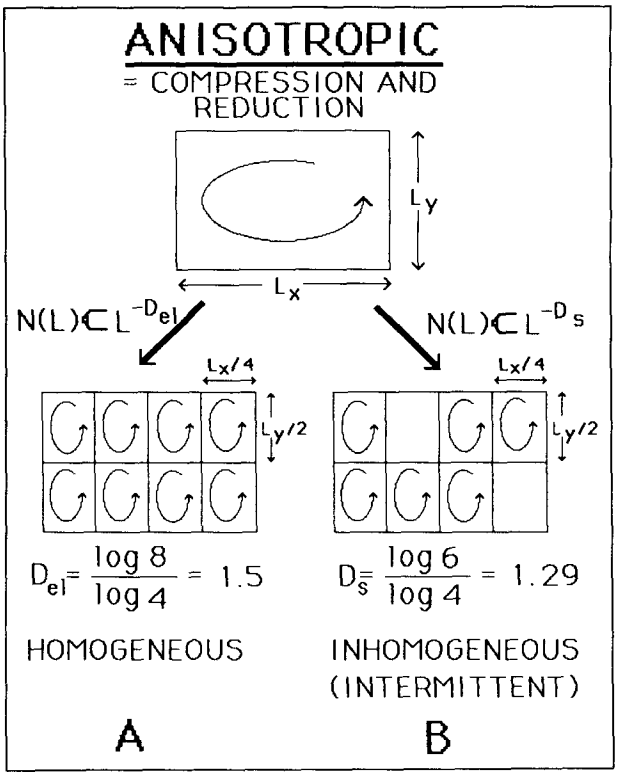

FIG. 5. As in Fig. 1 but for anisotropic cascades where the horizontal and vertical axes are divided by different factors (4 and 2 respectively). This defines a new exponent $H_z = \log 2/\log 4 = 1/2$ and elliptical dimension $D_{el} = 1 + H_z = 3/2$.

3. A theoretical framework for anisotropic and intermittent cascades—GSI

a. The elements of GSI

We have illustrated the nonlinear breakup of eddies using simple isotropic- and anisotropic-cascade schemes involving two components: 1) a rule specifying how eddies are transformed from one scale to another (or rather how their statistical properties are transformed), while 2) leaving the total energy flux invariant. More generally, we require two basic sets. The first set is a group of scale-changing transformations that define how the average eddy shapes change with scale. Attention is restricted here to an important class of scale-changing transformations that define a distance. By specifying the anisotropy and metric at each scale, the link between fluctuations of different sizes is provided.[12] The second set consists of elements that are measure invariant under the scale-changing group. They define the conserved quantities (e.g. energy flux) and provide the link between fluctuations of different intensities. In this subsection, it is shown how GSI gives precise meaning to each component, and generalizes them, allowing development beyond the unrealistic eddy shapes used so far. Although GSI leads to a number of consequences that are at first sight surprising, a closer look shows that they are supported by a wide body of empirical evidence. Theoretically, GSI is appealing, since it is a symmetry likely to be respected by solutions of the Navier-Stokes equations which govern fluid dynamics. For the full details of GSI, see Schertzer and Lovejoy (1985c). On a first reading, the rest of this subsection can be skipped without loss of continuity.

1) SCALE-CHANGE OPERATORS

Consider the operator T_λ that increases scales by a (positive) factor (for example, in Fig. 1, 4, or 5 it might transform eddies into subeddies). Obviously, the T_λ must satisfy certain properties:

1) They form a group: $T_\lambda T_\mu = T_\mu T_\lambda = T_{\lambda\mu}$ for all positive λ, μ.
2) They define *balls* $B_\lambda = T_\lambda (B_1)$ (c.f. Fig. 4) increasing with λ such that there exists a distance d satisfying: $d(x,x') \leq 2\lambda$, where x, and x' are vector elements of B_λ. In the case of isotropic scaling, T_λ reduces to λ (a pure dilation). The simplest anisotropic cases (called linear GSI, Fig. 4), are obtained by considering $T_\lambda = \exp(G \ln \lambda) = \lambda^G$ where G is a matrix called the generator of the group.

Although the derivation is technically quite involved, Schertzer and Lovejoy (1985b,c,d) show that when the

[12] Actually, Schertzer and Lovejoy (1985b,c) show that metric properties are not essential; eddies need only be measurable.

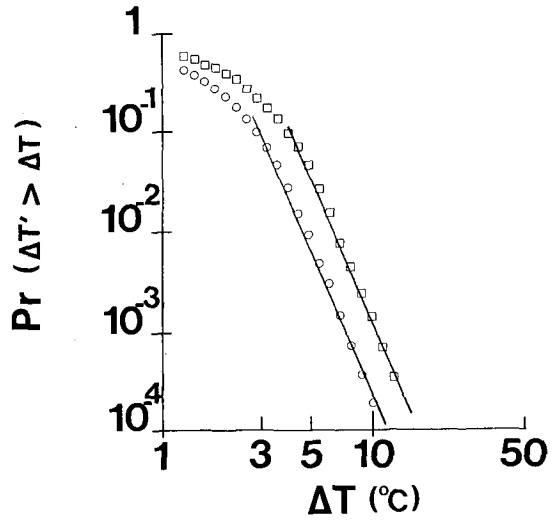

FIG. 6. The probability, $Pr(\Delta T' > \Delta T)$, of a random temperature difference, $\Delta T'$, exceeding a fixed threshold, ΔT. The squares are the daily differences of daily average temperatures at Macon (France) for the period 1951–81. The circles are for the corresponding temperatures averaged over 53 stations distributed all over France. This spatial averaging smooths out the fluctuations, hence the amplitudes are decreased. Note that because of scaling, the only difference is a constant factor (linear shift on this log-log plot). See Lovejoy and Schertzer (1985a) for a discussion.

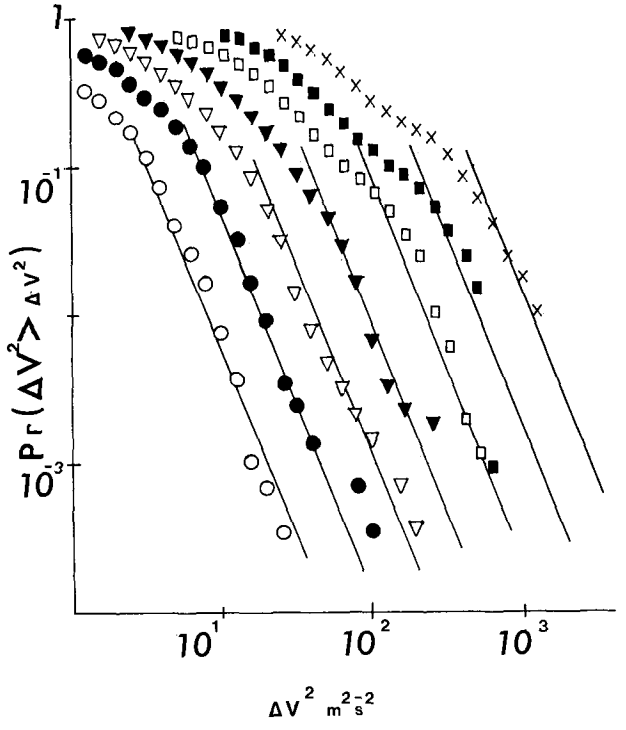

FIG. 7. The probability, $Pr(\Delta V^2 > \Delta v^2)$, of a random vertical wind shear squared, ΔV^2, exceeding a fixed threshold, Δv^2, for layers of thickness ΔZ. Symbols from left to right are for layers 50, 100, 200, 400, 800, 1600, and 3200 m thick. Data were obtained from 80 consecutive three-hourly high-resolution radiosondes in Landes, France, in 1975. The straight lines have slopes $(=\alpha_v/2) = 5/2$ $(\Rightarrow \alpha_v = 5)$ m and the regular spacing indicates scaling with $H \sim 3/5$ $(\Rightarrow \beta_v = 2H + 1 \sim 11/5)$. For details, see Schertzer and Lovejoy (1985a).

unit ball is a sphere, and when the symmetric part of **G** has eigenvalues greater than one, then T_λ satisfies these criteria. Thus a precise meaning is given to the expression "anisotropic scale invariance." Nonlinear transformations are necessary to deal with anisotropy that is position-dependent and involves the use of differential manifolds.

2) INVARIANT MEASURES

In GSI, the quantities of interest (e.g. ϵ) are mathematically measure invariant under the action of T_λ:

$$T_\lambda(\epsilon) = \lambda^D \epsilon,$$

where D is the dimension of the support of ϵ.[13] When ϵ is an energy flux, this expression can be read: "the energy flux through a region enlarged by the factor λ is λ^D times greater." If we consider the usual volume measure (e.g. *dxdydz*), it is scale invariant with $D = D_{el}$ (in general, $\neq 3$), where D_{el} is the anisotropic elliptical dimension introduced in Schertzer and Lovejoy (1983, 1984a):

$$D_{el} = \text{Trace } \mathbf{G} = \log det\ (T_\lambda).$$

b. Some physical consequences

Schertzer and Lovejoy (1985b, c) show that in general, measures invariant under GSI have the two closely related properties noted in Section 2c. First, they are multidimensional, and second, fluctuations of spatial averages of ϵ are hyperbolically distributed (as defined in Section 2c). This leads to a specific type of strong intermittency, called hyperbolic intermittency, characterized by the exponent α of the corresponding probability distribution. Note that α is conceptually quite different from β or D, which are defined irrespective of the probability distribution.

There is now much evidence (see, e.g., Figs. 6, 7, 8) supporting this kind of hyperbolic intermittency in the atmosphere. Some empirical values of the exponent α are: 5/3 for the rainfield (Lovejoy, 1981); 5, 10/3, 5/3, 1, and 1 for the velocity, buoyancy force, energy flux, Richardson number and buoyancy force–variance flux respectively (Schertzer and Lovejoy, 1985a); 5 for temperature (see Fig. 6; Ladoy *et al.*, 1985); and 1 for the radar reflectivity (Lovejoy and Schertzer, 1985c).

Whereas scale-invariant fluctuations have no characteristic length, hyperbolically intermittent fluctuations have no characterisic amplitude. In the extreme case where $\alpha < 2$, large fluctuations occur so frequently that the largest member of a sample of such fluctuations is always of the same order of magnitude as the sum of all the others in the sample.[14] Unlike the familiar case of quasi-Gaussian fluctuations, where the fluctuations rarely exceed two or three standard deviations and are thus all of the same order of magnitude, here the largest dominates the others no matter what the sample size. This phenomenon was first noted by Mandelbrot and Wallis

[13] The equality sign may be understood in different ways, e.g. deterministically, "almost surely," or as signifying equality of probability distributions, the latter being one of the most useful in meteorology.

[14] In general, if $h \sim \alpha$, this statement is true of the largest hth power of a sample as compared to the sum of all the other hth powers.

(1968), who named it the Noah effect after the extreme fluctuation responsible for the biblical flood. We shall see below that in accord with the richness of actual meteorological phenomena, fluctuations of this type are compatible with a wide diversity of structures. Figure 9 graphically shows how this effect can lead to the erroneous suggestion that a rain-rate time series is separated by a few sharp changes into different regimes.

Above, we noted that the moments (e.g. $\langle \bar{\epsilon}^h \rangle$) diverge for $h \geqslant \alpha$.[15] Empirical moments, which are averages of empirical values, are of course finite: divergence of moments simply means that the former increase without limit with increasing sample size. The bothersome "outliers" familiar to experimentalists are replaced by even larger outliers as the data base increases—no matter how large the sample size, we are plagued by a small number of extreme values contributing a large fraction of the moments. Ascribing the outliers to non-stationarity in the statistics and then eliminating them from the sample is both arbitrary and unwarranted. An important specific example is the ubiquity of outlier problems in cloud-seeding experiments which is probably linked to the low value of α in the rain field. Another experimental situation where we may expect hyperbolic intermittency to generate outliers is the boundary layer. There, experimentalists often calculate high-order moments in order to calibrate statistical closure models, and they are known to have problems getting their empirical averages to converge (Wyngaard, personal communication, 1984). The divergence of moments may also have simple consequences for empirical measurements of high-order structure functions (c.f. Schertzer and Lovejoy, 1983, 1984a) associated with the breakdown of the law of large numbers.

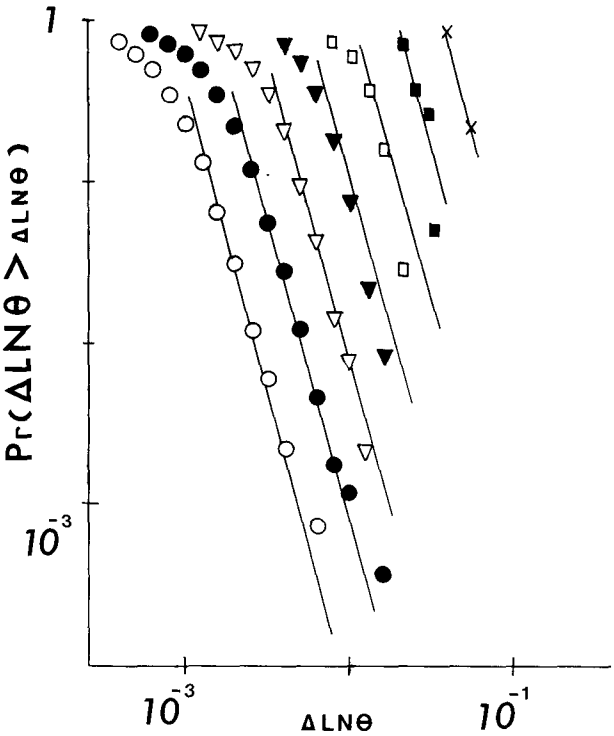

FIG. 8. As in Fig. 7, but for the probability $Pr(\Delta \ln\Theta > \ln\Delta\theta)$ of a random vertical (log) potential temperature difference $\Delta \ln\Theta$ exceeding a fixed threshold $\Delta \ln\theta$. The straight lines indicate $\alpha_{\ln\theta} \sim 10/3$, $H_{\ln\theta} \sim 9/10$.

4. The role of stochastic models

a. The fractal-sums-of-pulses process

Although primarily instructive in purpose, the preceding cascade schemes capture many of the salient features of the atmosphere: extreme variability, anisotropy, and scale invariance. To be of direct use, more-realistic models are clearly necessary. Researchers, motivated by empirical studies of the rain field (Lovejoy, 1981, 1982, 1983; Lovejoy and Schertzer, 1985d), developed the fractal-sums-of-pulses (FSP) process (Mandelbrot, 1984b; see Lovejoy and Mandelbrot, 1985, for the implementation in one, two and three dimensions), which is visually more realistic (see Figs. 10, 11, 12). In the FSP process, rain and cloud fields are simulated by adding many elementary shapes ("pulses") in a scale-invariant manner. The actual shapes used in the self-similar model discussed in Lovejoy and Mandelbrot (1985) were circles and annuli for horizontal cross sections, and spheres and spherical shells for the temporal evolution respectively (see Fig. 10b, c). Due to the Noah effect the strongest of these pulses dominates the others

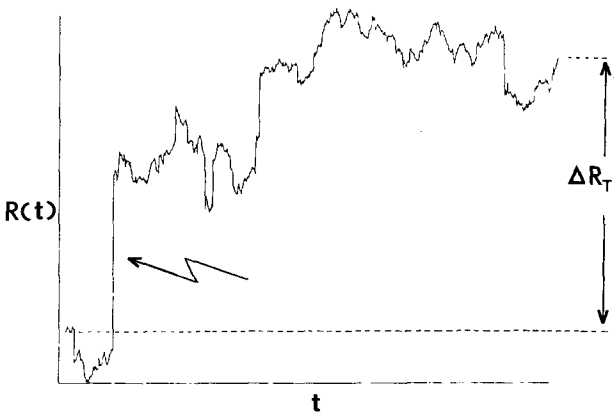

FIG. 9. Illustration of the Noah effect. A discrete rain-rate time series, $R(t)$, is modeled by the expression $R(t_i) = \sum_{j=1}^{i} \Delta R_j$ where the ΔR_j are independent, identically distributed random variables of the form $Pr(|\Delta R| > \Delta r) \propto \Delta r^{-\alpha}$ (with $\alpha = 5/3$ as determined from radar observations), which is the probability of a random change, ΔR, exceeding a fixed threshold, Δr. The signs of the ΔR were chosen randomly. The index i runs from 1 to 1300. The resulting $R(t)$ occasionally has such large "jumps" that over any interval, most of the total change in $R(t)$ is due to only one or two extreme changes, which thereby dominate the others. Here, the largest jump (indicated by the arrow) yields roughly two-thirds of the total change ΔR_T (indicated to the right).

[15] The divergence is a simple consequence of the hyperbolic tail of the distribution:

$$\langle \bar{\epsilon}^h \rangle = \int \bar{\epsilon}^h dPr = \int \bar{\epsilon}^h \bar{\epsilon}^{-\alpha-1} d\bar{\epsilon} \to \infty \qquad \text{for } h \geqslant \alpha.$$

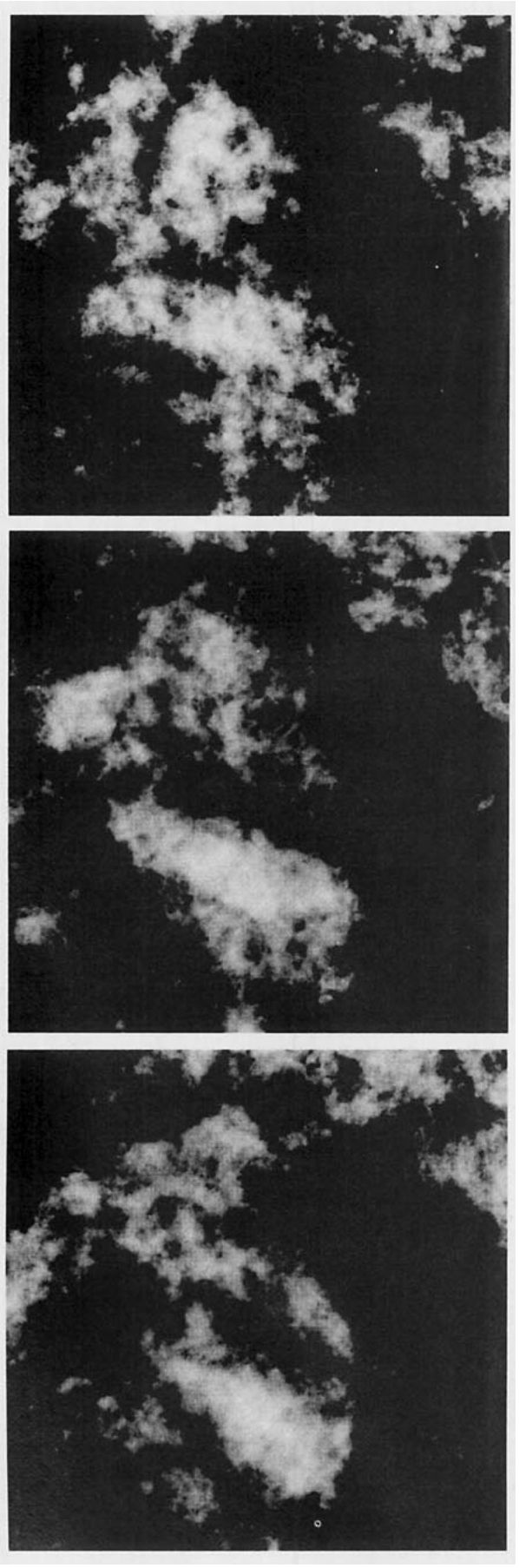

and thus subtly imposes its geometry. The shapes used in these figures are only the simplest possible.

The temporal evolution may be modeled by assuming Taylor's hypothesis of frozen turbulence, which states that temporal statistics are simply spatial statistics dimensionalized by an appropriate velocity factor; Brown and Robinson, 1979, empirically verify this hypothesis for distances up to 1000 km. Lovejoy and Schertzer (1985b) show how FSP models can be used to model both vertical stratification and the effect of the Coriolis force (see Figs. 3, 4). Although these models depend on only two basic radar-determined parameters (the scaling parameter H, which is related to the spectral exponent β, and the intermittency parameter α), they possess a number of realistic features including:

1) extreme variability over a wide range of scales;
2) realistic "complexity" of shapes (as measured by the fractal dimension of the perimeters);
3) the clustering of cells at all scales, including realistic distributions of rain and cloud areas;
4) the occasional appearance of bands and frontlike structures. For a discussion of the limitations of FSP models, as well as for several methods of overcoming them, see Lovejoy and Schertzer (1985b).

b. Some immediate applications

Models of this broad type are likely to be indispensible in many fields where extreme variability occurs over a wide range of scales. Stochastic fractal models provide a framework based on clear physical principles from which many of the problems in meteorology and of data anlaysis can be systematically studied. In stochastic modeling, the phenomenon of interest is assumed to be intrinsically extremely variable over a wide range of scales, and specific phenomena and processes are studied either directly or as perturbations to such a state. Mathematically, such models produce functions quite different from those accessible with the usual analytic techniques. Physically, phenomena are no longer smoothed out: discontinuities (e.g. fronts) are no longer treated as perturbations around a smooth basic state, nor are small-scale processes dealt with indirectly via parameterization schemes.

Obvious applications of these models include:

Mesoscale modeling. The standard deterministic-type mesoscale models can directly resolve only a small fraction of the range of the relevant scales (typically a factor of only 50). Fractal models deal with this problem in a simple way based on clear principles. Of course, the derivation of these principles from the equations (when they are known!) is a fundamental (and difficult) field of research. Stochastic models are useful not only in choosing between different theoretical possibilities, but also in evaluating their implications for the dynamics (particularly its intermittency and anisotropy).

The sampling problem. How are measurement errors affected by the density and frequency of measurements? The

FIG. 10. (left) Model of the temporal evolution of an isotropic rain field on an 800 × 800 point grid. The images are separated by a time equivalent to 80 pixels. The log rain intensity is shown by the shades in the figure—a black background (=no rain), with white being the most intense.

sampling and averaging properties of various combinations and arrangements of sensors can be studied directly by using stochastic simulations. The problem is compounded by the fact that in general all the statistical properties (including averages) of atmospheric fields depend on both the scale and the dimension over which they are averaged. Using radar data, Lovejoy and Schertzer (1985c) and Lovejoy *et al.* (1985) empirically show the strong scale and dimensional dependence of the rain field. They also analyze the 9563-station world meteorological surface network,[16] and find them to be clustered down to scales of ~1 km with dimension $D \sim 1.75$ instead of $D = 2$, which would correspond to a uniform network over the two-dimensional surface of the earth.[17] One consequence of this reduced dimension is the inability of the network to detect very sparse phenomena (perhaps tornadoes) having a dimension smaller than ~0.25 ($=2 - D$); this minimum dimension is called the dimensional resolution of the network. A related problem is that of interpolating network measurements on to a regular grid—this may be likened to deducing the structure on a plane ($D = 2$) from knowledge only along a line ($D = 1$).

Remote sensing. Remote-sensing devices generally integrate nonlinearly the fields of interest. This problem is quite significant—for example Lovejoy and Austin (1980) showed that in the estimation of rain from passive microwave sensors a bias of at least 30% and errors of at least ±160% result from this effect alone. Projects are already under way to use stochastic models of this type to solve remote-sensing problems (see e.g. Cahalan *et al.*, 1984). Calibration of remotely sensed data must take into account the different averaging and sampling scales and dimensions (see the preceding paragraph).

Nowcasting. Various short-term automatic forecasting procedures (e.g. Rainsat—Bellon *et al.*, 1981) already capitalize on the "stochastic memory" of the atmosphere by basing predictions on the assumption of continued uniform advection of raining areas. Stochastic fractal models provide an ideal context for systematically studying the relationship between temporal and spatial statistics, as well as the limits of predictability. For example, we expect that due to hyperbolic intermittency, forecast errors can be occasionally very large. It is therefore of interest to compare various forecast procedures on both data and the model, where their accuracy is more easily understood.

Hydrology. Stochastic models of rain involving various time and space characteristics have long been used in hydrol-

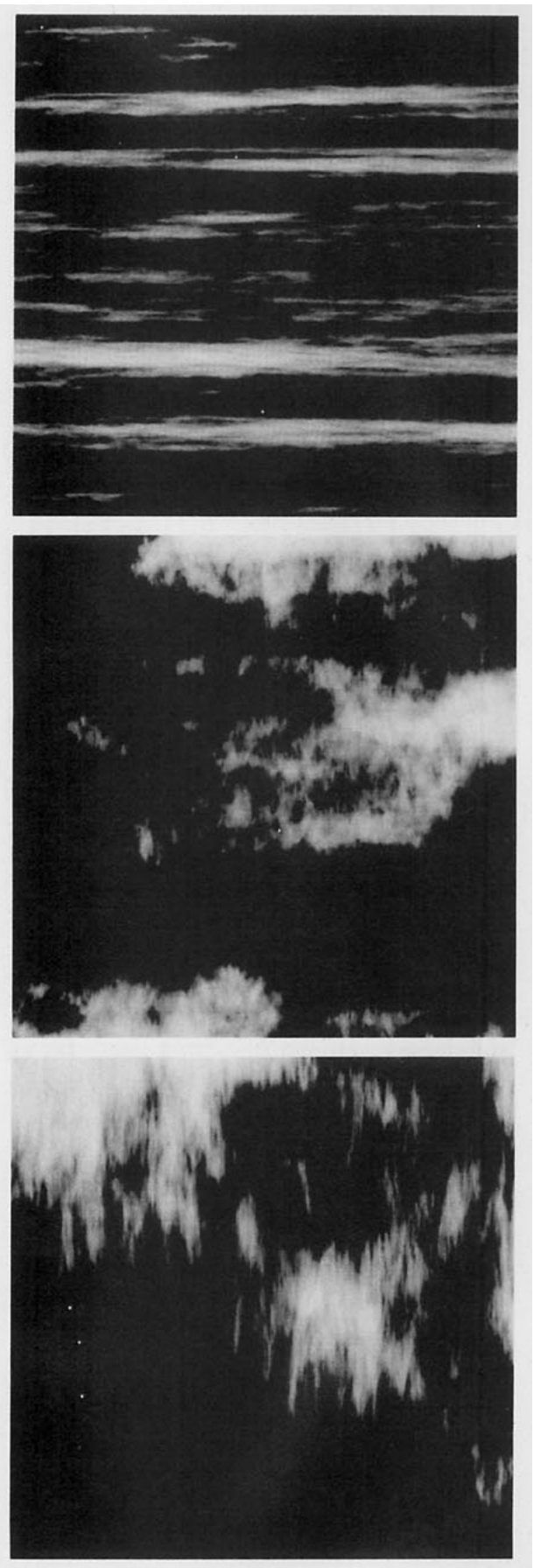

FIG. 11. (right) Model of a rain cross section on a 400 × 400 grid. Going from top to bottom we "zoom" in by factors of 100 (top to middle) and 10 (middle to bottom) on random sections. At one extreme (top), only the overall horizontal stratification is visible, while at the other (magnified 1000 times), only the intense rain "shafts" can be seen. The cover illustration corresponds to a random section selection falling between the top and middle parts of the figure (a 10-times "zoom" on the top rain cross section).

[16] These are stations that the World Meteorological Organization lists as recording at least one meteorological observation every 12 hours. For further information see Lovejoy *et al.*, 1985.

[17] Other analyses by the authors and P. Ladoy also find $D \sim 1.8$ for the 3943 climatological stations in France, down to about 10 km and $D \sim 1.5$ for the 414 meteorological stations in Canada down to ~30 km.

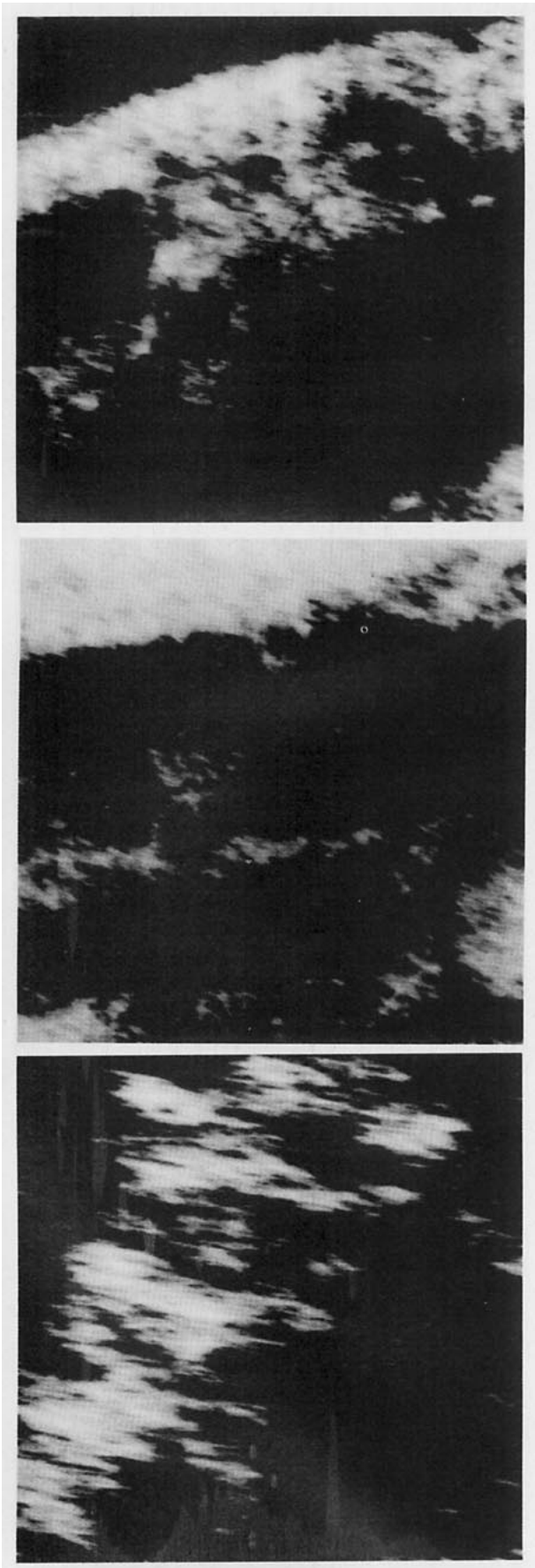

ogy (see e.g. the review by Waymire and Gupta, 1981). Fractal models should greatly extend the range of scales over which such models may be useful (Waymire, 1984).

Climatology. Climatological time scales are best defined as limits of scaling regimes. For example, Lovejoy and Schertzer (1985a) use hemispherically averaged temperatures and paleotemperatures to show that, at least for scales between five and 40 000 years, these temperatures are scaling, with the exponent β fully compatible with the amplitude and frequency of the interglacials. However, the behavior of local temperatures is different, and stochastic models may prove useful in understanding this difference.

The study of NWP systems. Schertzer *et al.* (1983) proposed that the "stochastic coherence" of NWP systems be studied by comparing the measured values of β and α against those generated by NWP systems. In this way it is possible to systematically determine whether or not the complex set of operations they involve have a tendency to artificially create or destroy disturbances of a given size or to artificially suppress disturbances of large intensity (e.g., fronts).

5. Conclusions

Supported by simple stochastic fractal models, we have argued that the scaling, anisotropy, and extreme intermittency of the mesoscale may be understood in terms of a symmetry principle called generalized scale invariance. Although the work described here is only a modest beginning and leaves many important questions unanswered, we believe that there are at least three compelling reasons to believe that GSI is relevant to atmospheric dynamics. First, a vast body of data, especially from spectra and probability distributions, gives very solid support to both scaling and hyperbolic intermittency. Second, a growing body of theory suggests, but not yet proves, that many nonlinear systems (of which the Navier-Stokes equations are the prototypical example) can be scale invariant over wide ranges, and thereby respect GSI. The third reason is the surprising success of simple fractal models such as the FSP process in simulating, not only statistically but also visually, both rain and cloud fields. Apparently, fields with extreme intermittency over a wide range of scales are by nature rife with meteorological-like features, including lines, bands and clusters, texture, and complexity. Although still at a primitive stage, these models can already be used in mesoscale modeling, sampling problems, remote sensing, nowcasting, hydrology, climatology, and in the study of NWP systems.

In our opinion, the fact that the notions of scaling, fractals, and intermittency, which were primarily developed in the context of nonlinear dynamics, can—after necessary elaboration—be profitably used in concrete meteorological problems, is a witness to the enormous potential for common advances (e.g. Hentschel and Procaccia [1984] or Levitch *et al.* [1984]).

FIG. 12. (left) Model of a horizontal rain cross section with varying degrees of differential rotation. In one case (bottom), the rotation was chosen so that the largest and the smallest scales are nearly perpendicular, yielding (to use the official nomenclature) the appearance of cirrus fibratus vertibratus clouds.

Acknowledgments. We especially benefitted from discussion with G. Austin, T. Gal-Chen, D. Lilly, B. Mandelbrot, R. Peschanski, and J. Peyrière. We also acknowledge R. Cahalan, C. Gauthier, V. Gupta, G. Hentschel, J. Herring, E. Hopfinger, P. Muller, I. Procaccia, M. Rafy, E. Waymire, and J. Wyngaard. Shaun Lovejoy would like to thank B. Mandelbrot and the T. Watson Research Center, IBM, for hospitality during the production of most of the simulations shown in this paper. Daniel Schertzer thanks the Aspen Center for Physics for hospitality during the summer of 1982. This work was partially supported by the Centre National de la Recherche Scientifique (ATP-RA (184) 16). Figure 10 (a,b, and c) is used by permission of *Tellus*.

References

Antonia, R. A., B. R. Satyaprakash, and A. J. Chambers, 1982: Reynolds number dependence of velocity structure functions in turbulent shear flows. *Phys. Fluids,* **25,** 29–37.

Batchelor, G. I., and A. A. Townsend, 1949: The nature of turbulent motion of large wave numbers. *Proc. Roy. Meteor. Soc.,* **A199,** 238.

Bellon, A., S. Lovejoy, and G. L. Austin, 1980: A short-term precipitation forecasting procedure using combined radar and satellite data. *Mon. Wea. Rev.,* **108,** 1554–1566.

Brachet, M. E., D. I. Meiron, S. A. Orszag, B. G. Nichkel, R. H. Morf, and U. Frisch, 1983: Small-scale structure of the Taylor-Green vortex. *J. Fluid Mech.,* **130,** 411.

Brown, P. S., and G. D. Robinson, 1979: The variance spectrum of tropospheric winds over Eastern Europe. *J. Atmos. Sci.,* **36,** 270–286.

Cahalan, R., W. Wiscombe, and J. H. Joseph, 1984: Fractal clouds from *Landsat* imagery. NASA Internal Report, Greenbelt, Md., 32 pp.

Chorin, A. J., 1981: Estimates of intermittency, spectra and blow-up in turbulence. *Commun. Pure Appl. Math.,* **34,** 853.

Frisch, U., P. L. Sulem, and M. Nelkin, 1978: A simple dynamical model of intermittent fully-developed turbulence. *J. Fluid Mech.,* **87,** 719–724.

Grassberger, P., 1983: Generalized dimensions of strange attractors. *Phys. Lett.,* **97A,** 227–230.

Hentschel, H. G. E., and I. Procaccia, 1983: The infinite number of generalized dimensions of fractals and strange attractors. *Physica,* **8D,** 435–444.

——, and ——, 1984: Relative diffusion in turbulent media: The fractal dimension of clouds. *Phys. Rev.,* **A29,** 1461–1470.

Kahane, J. P., 1976: Mesures et dimensions. *Turbulent and Navier-Stokes Equation,* R. Teman, Ed., Springer-Verlag, Berlin, 76–84.

——, 1985: *Some Random Series of Function,* 2nd ed. Cambridge University Press, Cambridge, (in press).

Kolmogorov, A. N., 1941: Local structure of turbulence in an incompressible liquid for very large Reynolds numbers. *C.R. Acad. Sci.,* **30,** 299–301.

Ladoy, P., S. Lovejoy, and D. Schertzer, 1985: Une étude de l'invariance locale globale des températures climatologiques. *La Météorologie* (submitted).

Levitch, E., B. Levitch, and A. Tsinober, 1984: Helical structures, fractal dimensions and renormalisation group approach in homogeneous turbulence. *Turbulence and Chaotic Phenomena in Fluids,* T. Tatsumi, Ed., North-Holland, Amsterdam, 309–317.

Lilly, D. K., 1983: Meso-scale variability of the atmosphere. *Meso-scale Meteorology—Theories, Observations and Models.* D. K. Lilly and T. Gal-Chen, Eds., D. Reidel, New York, 13–24.

Lovejoy, S., 1981: A statistical analysis of rain areas in terms of fractals. *Prepr., 20th Conf., Radar Meteorology,* Boston, American Meteorological Society, 476–484.

——, 1982: The area-perimeter relationship for rain and cloud areas. *Science,* **216,** 185–187.

——, 1983: La géométrie fractale des nuages et des regions de pluie et les simulations aléatoires (The fractal geometry of cloud and rain zones with random simulations). *Houille Blanche,* **516,** 431–436.

——, and G. L. Austin, 1980: The estimation of rain from satellite-borne microwave radiometers. *Quart. J. Roy. Meteor. Soc.,* **106,** 255–276.

——, and B. Mandelbrot, 1985: Fractal properties of rain and a fractal model. *Tellus* **37A,** 209–232.

——, and D. Schertzer, 1985a: Scale invariance in climatological temperatures and the spectral plateau. *Ann. Geophysicae.* (in press).

——, and ——, 1985b: Generalized scale invariance in the atmosphere and fractal models of rain. *Water Resour. Res.* **21,** 1233–1250.

——, and ——, 1985c: Extreme variability, scaling and fractals in remote sensing: Analysis and simulation. *Remote Sensing in Geophysics,* P. Muller, Ed., Taylor and Francis (in press).

——, and ——, 1985d: Rainfronts, fractals and rainfall simulations. *Hydrological Applications of Remote Sensing and Remote Data Transmission.* Proceedings of the Hamburg Symposium, 1983, IAHS Publ. No. 145, (in press).

Lovejoy, S., D. Schertzer, and P. Ladoy, 1985: Fractal characterization of inhomogeneous measuring networks. *Nature,* (in press).

Mandelbrot, B., 1974: Intermittent turbulence in self-similar cascades: Divergence of high moments and dimension of the carrier. *J. Fluid Mech.,* **62,** 331.

——, 1982: *The Fractal Geometry of Nature.* Freeman and Co., New York, 461 pp.

——, 1984a: Fractals in physics: Squig clusters, diffusions, fractal measures and the unicity of fractal dimensionality. *J. Stat. Phys.,* **34,** 895–930.

——, 1984b: Fractal sums of pulses and new random variables and functions. [Available from the author—Mathematics Dept., Harvard University.]

——, J. R. Wallis, 1968: Noah, Joseph and operational hydrology. *Wat. Resour. Res.,* **4,** 909–918.

Monin, A. S., 1972: *Weather Forecasting as a Problem in Physics.* MIT Press, Cambridge, Mass., 260 pp.

Novikov, E. A., and R. Stewart, 1964: Intermittency of turbulence and spectrum of fluctuations of energy dissipation. *Izv. Akad. Nauk. SSSR Ser. Geofiz.,* **3,** 408.

Parisi, O., and U. Frisch, 1985: A multifractal model of intermittency. *Turbulence and Predictability in Geophysical Fluid Dynamics and Climate Dynamics,* M. Ghil, R. Benzi, and G. Parisi, Eds., North-Holland, Amsterdam, p. 84.

Richardson, L. F., 1922: *Weather Prediction by Numerical Process.* Republished by Dover, New York, 1965, 160 pp.

——, 1926: Atmospheric diffusion shown on a distance neighbor graph. *Proc. Roy. Soc. London,* **A110,** 709.

Schertzer, D., and S. Lovejoy, 1983: On the dimension of atmospheric motions. *Preprints, IUTAM Symp. on Turbulence and Chaotic Phenomenon in Fluids,* Kyoto, Japan, IUTAM, 141–144.

——, and ——, 1984a: On the dimension of atmospheric motions. *Turbulence and Chaotic Phenomena in Fluids,* T. Tatsumi, Ed., North-Holland, 505–512.

——, and ——, 1984b: Les fractales dans l'atmosphère. *Sci. Tech.,* **5,** 68–72.

——, and ——, 1985a: The dimension and intermittency of atmospheric dynamics. *Turbulent Shear Flow,* **4,** B. Launder, Ed., Springer, New York, 7–33.

——, and ——, 1985b: Generalized scale invariance in turbulent phenomena. *P. C. H. Journal* **6,** 623–635.

——, and ——, 1985c: Generalized scale invariance: Symmetrics, measures, and dimension in anisotropic spaces. *J. Phys.* (submitted).

Schertzer, D. and S. Lovejoy, 1985d: Generalized scale invariance and anisotropic intermittent fractals. *Fractals in Physics*, E. Pietronero, Ed., North-Holland (in press).

——, ——, G. Therry, J. Coiffier, Y. Ernie, and J. Clochard, 1983: Are current NWP systems stochastically coherent? *Preprints, IAMAP/WMO Symp. Maintenance of the Quasi-Stationary Components of the Flow in the Atmosphere and in Atmospheric Models*, Paris. WMO, Geneva, 325–328.

Van der Hoven, J., 1957: Power spectrum of horizontal wind speed in the frequency range from 0.0007 to 900 cycles per hour. *J. Meteor.*, **14**, 160–164.

Waymire, E., 1985: Scaling limits and self-similarity in precipitation fields. *Wat. Resour. Res.* **21**, 1251–1265.

——, and V. K. Gupta, 1981: The mathematical structure of rainfall representations, parts 1–3. *Wat. Resour. Res.*, **17**, 1261–1294.

Wyngaard J., 1983: *Mesoscale Meteorology—Theories, Observations and Models.* Lilly and Gal-Chen, Eds. D. Reidel, New York, 216–224.

Yaglom, A. M., 1966: The influence of the fluctuation in energy dissipation on the shape of turbulent characteristics in the inertial interval. *Sov. Phys. Dokl.*, **2**, 26. •

announcements (*continued from page 15*)

30 April–2 May 1986. An anticipated 500 members of the marine community are expected to attend the international marine symposiums to be held from 30 April to 2 May 1986 in New Orleans, Louisiana. The symposium is sponsored by the Marine Technology Society with participation from a number of cooperating organizations. The objective of the symposium will be to provide a mechanism for the exchange of ideas and information relating to all aspects of marine data. Jerry C. McCall, director of the National Data Buoy Center, and Capt. James E. Koehr, commander of the Naval Oceanographic Command, will cochair the event at the Hyatt Regency Hotel, the symposium site. For further information contact the University of Southern Mississippi, Gulf Park, Long Beach, MS 39560; telephone (601) 865-4508.

17–24 May 1986. The Royal Meteorological Society is sponsoring a field-study weather course entitled Weather Under Sail on 17–24 May 1986. The course includes sailing in the English Channel. Participants will learn how to sail, how to measure weather elements, and how to use weather forecasts in plotting the boat's course.

June 1986. The Geophysical Institute of the Faculty of Natural Sciences and Mathematics at the University of Zagreb, Yugoslavia, is celebrating its 125th anniversary with a symposium in June 1986. The Symposium On Observations and Modelling in Geophysics will be conducted in English and in the languages of Yugoslav nations. For additional information, contact the Geophysical Institute, Faculty of Natural Sciences and Mathematics, University of Zagreb, P.O. Box 224, 41000 Zagreb, Yugoslavia; telephone 41-42022.

5–6 June 1986. The 43rd annual meeting of the Eastern Snow Conference will be held in Hanover, New Jersey, on 5–6 June 1986. Papers can be sent to Jean-Louise Bisson, Hydro Quebec, 9th Floor, 2 Compexe Des Jardins, Montreal, P.Q. H2Z 1A4, Canada.

22–27 June 1986. The 79th Air Pollution Control Association Annual Meeting & Exhibition will be held in Minneapolis, Minnesota on 22–27 June 1986. The technical sessions (23–27 June) and the exhibition (24–26 June) will cover the full spectrum of air-pollution control and hazardous-waste management technology. One- and two-day continuing-education courses are scheduled for 21–22 June, and two-hour refresher courses will be given on the evening of 24 June. For more information contact the Air Pollution Control Association, P.O. Box 2861, Pittsburgh, PA 15230; telephone (412) 232-3444.

8–15 August 1986. The Royal Meteorological Society is sponsoring a course on understanding weather that will take place in Yorkshire, England, from 8–15 August 1986. A full week's program of talks, outdoor work, and films will include wind and temperature measurements from sailboats, a forecasting competition, and the launching and tracking of hydrogen-filled balloons. For further details on the course, write to the Executive Secretary, Royal Meteorological Society, James Glaisher House, Grenville Place, Bracknell, Berkshire, UK RG12 1BX.

Deadlines Calendar

Fellowships, grants, etc.

15 June 1986	Macelwane Annual Award (this issue, p. 45)
15 June 1986	Hanks and Orville Scholarships (this issue, p. 45)

Other

15 January 1986	applications for 1986 Resident, Cooperative, and Postdoctoral Research Associateship Programs (December BULLETIN, p. 1505)
17 January 1986	applications for Ford Foundation postdoctoral fellowships for minorities (December BULLETIN, p. 1505)
1 February 1986	papers for the Conference on Precision Electromagnetic Measurements (December BULLETIN, p. 1510)
13 February 1986	requests for NCAR aircraft (October BULLETIN, p. 1304)
14 February 1986	reservations for the Eleventh Annual Northeastern Storm Conference (this issue, p. 15)
15 February 1986	nominations for SWE Distinguished Engineering Educator Award (December BULLETIN, p. 1505)
1 March 1986	requests for NCAR field-observing support (October BULLETIN, p. 1331)
31 March 1986	completed manuscripts of accepted papers for U.S. EPA/EMSL/APCA Symposium on Measurement of Toxic Air Pollutants (November BULLETIN, p. 1395) •